

This work was written as part of one of the author's official duties as an Employee of the United States Government and is therefore a work of the United States Government. In accordance with 17 U.S.C. 105, no copyright protection is available for such works under U.S. Law.

Public Domain Mark 1.0

<https://creativecommons.org/publicdomain/mark/1.0/>

Access to this work was provided by the University of Maryland, Baltimore County (UMBC) ScholarWorks@UMBC digital repository on the Maryland Shared Open Access (MD-SOAR) platform.

Please provide feedback

Please support the ScholarWorks@UMBC repository by emailing scholarworks-group@umbc.edu and telling us what having access to this work means to you and why it's important to you. Thank you.

A study of tropospheric ozone column enhancements over North America using satellite data and a global chemical transport model

Qing Yang,¹ Derek M. Cunnold,^{1,2} Yunsoo Choi,³ Yuhang Wang,¹ Junsang Nam,¹ Hsiang-Jui Wang,¹ Lucien Froidevaux,³ Anne M. Thompson,⁴ and P. K. Bhartia⁵

Received 8 June 2009; revised 9 October 2009; accepted 4 December 2009; published 30 April 2010.

[1] Tropospheric ozone columns (TCOs) have been calculated from the differences between the Aura Ozone Monitoring Instrument (OMI) Total Ozone Mapping System (TOMS) total ozone (level 2 version 3) and the Aura Microwave Limb Sounding (MLS) measurements of stratospheric ozone (version 2.2). These OMI-MLS TCOs were compared against ozonesonde measurements from the Intercontinental Chemical Transport Experiment (INTEX) Ozonesonde Network Study (IONS) campaign over North America in spring and summer, 2006. The OMI-MLS potential vorticity mapped TCOs are smaller than IONS TCOs by 5.9 DU (9.9 ppb when expressed as volume mixing ratio) with a standard deviation of the differences of 8.4 DU (14.4 ppb) and a standard error of the mean differences of approximately 0.5 DU (0.7 ppb). Compared to previously published versions, these OMI-MLS TCOs are an additional 2 DU smaller relative to ozonesonde measurements. The extra 2 DU arises from changes in OMI (~ -3 to -6 DU) and MLS (-1 to 3 DU), giving a net change of -2 DU. OMI-MLS TCOs derived using OMI Differential Optical Absorption Spectroscopy (DOAS) show similar differences in summer, but these TCOs are smaller than the sondes by only 2 DU (5 ppb) in spring. OMI-MLS TCOs derived from TOMS total ozone retrievals lead to better results when validated against IONS data, with less noise and a better seasonal consistency. Tropospheric ozone columns were also compared to those from GEOS-Chem model simulations in main distribution features. In the spring and summer of 2005 and 2006, the most dominant enhancement features are a tongue of enhancement stretching from around Yellow Sea northeastward into the Pacific and an enhancement band over the North America centered over the eastern United States and the adjacent ocean. The OMI-MLS TCO enhancements over the western Pacific and over the eastern United States increased from March to June and then decreased. In the GEOS-Chem model simulations, the monthly variation tendency is similar to that of satellite data over the west Pacific but the decrease tendency from June into August over eastern United States is less dramatic. A springtime TCO enhancement event of a few days duration over coastal California was investigated to demonstrate the ability of OMI-MLS mapped TCO columns in capturing ozone enhancements associated with stratospheric intrusions and trans-Pacific transport. Tagged ozone model simulations support the stratospheric contributions to the high TCOs over coastal California and over the Baja peninsula, and meteorological fields indicate that the stratospheric intrusions are associated with Rossby wave breaking events. Furthermore, back trajectory studies and comparisons of GEOS-Chem standard simulations and sensitivity runs with Asia anthropogenic emissions turned off provide evidence that the high tropospheric ozone columns over coastal California near Santa Barbara, California, has been influenced by cross-Pacific transport. Two-day-average maps of tropospheric ozone columns from Aura OMI-MLS TCOs also indicate cross-Pacific propagating features.

¹School of Earth and Atmospheric Sciences, Georgia Institute of Technology, Atlanta, Georgia, USA.

²Deceased 18 April 2009.

³Jet Propulsion Laboratory, California Institute of Technology, Pasadena, California, USA.

⁴Department of Meteorology, Pennsylvania State University, University Park, Pennsylvania, USA.

⁵Laboratory for Atmospheres, NASA Goddard Space Flight Center, Greenbelt, Maryland, USA.

Citation: Yang, Q., D. M. Cunnold, Y. Choi, Y. Wang, J. Nam, H.-J. Wang, L. Froidevaux, A. M. Thompson, and P. K. Bhartia (2010), A study of tropospheric ozone column enhancements over North America using satellite data and a global chemical transport model, *J. Geophys. Res.*, *115*, D08302, doi:10.1029/2009JD012616.

1. Introduction

[2] Although ozone is a trace gas, it plays an important role in atmospheric chemistry and climate variability. Transport from the stratosphere is one of the major sources of ozone in the troposphere according to observations [e.g., Thompson *et al.*, 2007a, 2007b] and model studies [e.g., Roelofs and Lelieveld, 1997; Pfister *et al.*, 2008]. Even though more stratospheric flux during spring has been reported, frequency of the stratospheric intrusion is also significant at other seasons [Thompson *et al.*, 2007a, 2008, and references therein]. Thompson *et al.* [2007a] arrived at an average value of 23% for the stratospheric contribution to summertime tropospheric ozone based on measurements at 7 North America sites during Intercontinental Transport Experiment (INTEX) Ozone Sonde Network Study in July–August 2004 (IONS-4). Model budgets from Pfister *et al.* [2008] showed an overall of 26% contribution from stratospheric ozone, which is only slightly higher than the budget (20%) they obtained from IONS-4 sites using the “laminar identification method.” Mechanisms in different scales are associated with the transport of ozone from the stratosphere down to the troposphere including large-scale wave-induced forcing, synoptic-scale mechanisms, and small-scale mechanisms such as extratropical cyclones (cyclogenesis) and tropopause folding [Holton *et al.*, 1995; Mahlman, 1997; Zanis *et al.*, 2003]. Rossby wave breaking is one of the important mixing mechanisms near the tropopause [Postel and Hitchman, 1999].

[3] Another important tropospheric ozone source is the transport of trace gases within the troposphere. Because of the rapid economic development in East Asia, large amounts of ozone and ozone precursors are produced or emitted there. Trans-Pacific transport of Asian pollution has been found to influence the ozone and aerosol air quality in the United States during spring [Heald *et al.*, 2006; Hudman *et al.*, 2004; Yienger *et al.*, 2000]. Trans-Pacific transport of ozone pollution mostly takes place in the free troposphere where winds are strong and the ozone lifetime is long [Hudman *et al.*, 2004, and references therein]. After the pollutants have been mixed into the free troposphere, it takes about 5–10 days for the pollution to cross the Pacific Ocean [Heald *et al.*, 2003, and references therein]. Model simulations and observational campaigns suggest that trans-Pacific transport episodes often peak in spring with three to five large Asian pollution events reaching the western United States [Liang *et al.*, 2004; Yienger *et al.*, 2000].

[4] The mixture of different ozone sources makes it challenging to understand ozone variability in the troposphere. The integration of recent satellite measurements and model simulations is a promising approach for providing additional insights into the study of tropospheric ozone [e.g., Ziemke *et al.*, 2006; Schoeberl *et al.*, 2007]. Yang *et al.* [2007] implemented a potential vorticity (PV)-ozone mapping technique to increase the spatial and temporal coverage of the Microwave Limb Sounder (MLS) data, and tropospheric ozone columns (TCOs) were calculated from dif-

ferences between Aura Ozone Mapping Instrument (OMI) total ozone columns and MLS mapped stratospheric ozone columns. Validation showed these OMI-MLS TCOs have a low bias of ~ 4 DU relative to tropospheric columns measured by ozonesondes, which agreed with the results of Ziemke *et al.* [2006] and Schoeberl *et al.* [2007]. TCOs derived by Yang *et al.* [2007], combined with regional chemical transport model calculations, have been used by Choi *et al.* [2008a] to study a spring to summer northward migration of high tropospheric ozone values over the western North Atlantic.

[5] This paper is organized as below. In section 3, the quality of the OMI-MLS TCOs derived using the Yang *et al.* [2007] approach but using the more recent retrieval versions of Aura OMI and MLS ozone measurements are validated against TCOs from IONS ozonesondes, TES, GEOS-Chem simulations, and the OMI-MLS TCOs derived based on a trajectory mapping approach; In section 4, the variability of the OMI-MLS mapped TCOs were compared against those from GEOS-Chem in spring and summer over the Pacific and over the North America; In section 5, the ability of the derived OMI-MLS mapped TCOs in capturing ozone enhancements associated with trans-Pacific transport and stratospheric intrusions are demonstrated through the study of a spring TCO enhancement event. The enhancement event was associated with a strong TCO enhancement over the Baja peninsula of Mexico and over the west coast of the United States in 2005. Even though GEOS-Chem simulations are included, this paper is a satellite product dominated paper. As such, the case study analysis is not as in depth as a paper focusing on using the models.

2. Data

2.1. Satellite Data: OMI-MLS TCOs

[6] The tropospheric ozone columns in this paper were computed from the differences between “clear sky” OMI total ozone columns and MLS measurements of stratospheric ozone, as in the paper by Yang *et al.* [2007], but using current versions of MLS (version 2.2) and OMI data. The TCOs differ according to whether OMI Differential Optical Absorption Spectroscopy (DOAS) total ozone (level 2 collection 3) retrievals or OMI Total Ozone Mapping System (TOMS) total ozone (level 2 version 3) retrievals were used. The TOMS algorithm is based on the algorithm used for the many years of TOMS measurements which are measured at 6 discrete wavelengths rather than continuously measured at moderate spectral resolution as in OMI. Instead of using cloud top pressure from a climatology, the TOMS level 2 version 3 algorithm uses the effective cloud top pressure derived from Raman scattering in OMI radiances [Joiner and Vasilkov, 2006]. The OMI DOAS level 2 collection 3 algorithm derives total ozone column by fitting the OMI radiances using the DOAS approach; it uses the effective cloud top pressure derived from OMI O_2-O_2 absorption band [Acarreta *et al.*, 2004]. The majority of this paper uses

the OMI TOMS total ozone retrievals. However, differences between the TOMS and DOAS TCOs are initially estimated. For each of the two sets, three sets of OMI-MLS TCOs (coincident, 2-D interpolated, and PV mapped TCOs) were produced.

[7] The definition of a clear sky condition differs between OMI TOMS and OMI DOAS retrievals. For OMI TOMS total ozone, the clear sky condition was defined by a reflectivity of less than 30% based on the OMI 360 nm reflectivity provided in the level 2, version 3 OMI TOMS products (see Yang *et al.* [2007] for justification). When using OMI DOAS products, a value of < 0.50 in the 'CloudRadianceFraction' was used as the clear sky condition (Pepijn Veefkind, personal communication, 2008). 'CloudRadianceFraction' is the fraction of the light that comes from the cloudy area in a ground pixel, and this parameter was also used in the DOAS retrieval algorithm to determine how much ozone is added under the clouds. It is important to note that climatological values of ozone are used for the below cloud values in both retrieval algorithms.

[8] The TCOs were calculated both in DU and in volume mixing ratio (VMR). The conversion of TCOs from DU to VMR is made by dividing by the pressure difference (in hPa) between surface and the tropopause, followed by multiplication by a constant (0.7889) [Ziemke *et al.*, 2006]. The TCOs expressed in VMR have the advantage of eliminating the TCO variations caused by changes in the amount (weight more specifically) of air in the tropospheric columns associated with, for example, topography effects. Thus, plots in this paper are presented with TCOs expressed in volume mixing ratio. For coincident and 2-D interpolated TCOs, daily means of the pressure differences were used because the OMI and MLS measurements were not made at exactly the same times. The accuracy of these TCOs expressed in VMR may, however, inevitably be slightly compromised when the surface and tropopause pressures have large variations in a day. Unless otherwise stated, the tropopause heights and surface pressures used in the calculation of TCOs in this paper were directly obtained from National Center for Environmental Prediction/National Center for Atmospheric Research (NCEP/NCAR) reanalysis 1 data set.

[9] Descriptive details of each of the three sets of derived TCOs are given in the auxiliary material and in the paper by Yang *et al.* [2007].¹

2.2. Satellite Data: TES Ozone Measurements

[10] The Tropospheric Emission Spectrometer (TES) is an infrared, high-resolution, Fourier transform spectrometer, which is on board the Aura satellite providing ozone measurements in the troposphere [Beer, 2006]. TES operates in global survey and special observation modes. This study used the standard nadir viewing TES products produced from the global survey mode. When comparing TES total tropospheric ozone columns against OMI-MLS columns, the effect of the TES averaging kernels has been assumed to be small because the TES vertical resolution is about 6–7 km.

2.3. IONS Data

[11] The INTEX-B Ozone Sonde Network Study in 2006 (IONS-06) was conducted for the purpose of quantify intracontinental and intercontinental pollution transport [Thompson *et al.*, 2008]. With regular measurements over 15 North America sites and over 700 high-resolution ozone profiles extending from surface to midstratosphere (~35 km), IONS-06 provides a valuable data set for Aura instrument validation as well as for evaluation of models [Thompson *et al.*, 2008]. These ozonesonde measurements were located mostly between 20°N and 60°N over North America, and they possessed the advantage of being close in times and locations to the Aura measurements.

2.4. GEOS-Chem Model Simulations

[12] This study uses version 8-01-01 of the GEOS-Chem global 3-D chemical transport model (http://wiki.seas.harvard.edu/geos-chem/index.php/GEOS-Chem_v8-01-01) which is driven by assimilated meteorological observations from the Goddard Earth Observing System (GEOS-5) from the NASA Global Modeling and Assimilation Office (GMAO). The horizontal resolution of GEOS-Chem is $2^\circ \times 2.5^\circ$ latitude by longitude and the model has 47 vertical layers between the surface and 0.01 mb. Detailed O₃-NO_x-VOC-aerosol simulations were made for spring and summer in both 2005 and 2006. A detailed description and evaluation of the GEOS-Chem model has been reported by Bey *et al.* [2001] and Park *et al.* [2004]. The V8-01-01 has substantially improved the lightning simulations. The flash rate is spatially constrained to the climatological distribution and magnitude is based on OTD (Optical Transient Detector)/LIS (Lightning Imaging Sensor) observation; over extratropics, the NO_x yields are from the Hudman *et al.* [2007] constraint (500 mol/flash) (Lee Thomas Murray, personal communication, 2009). The National Emission Inventory of the U.S. Environmental Protection Agency (EPA), constructed for 1999 emission inventory (EPA-NEI 99) were used for the anthropogenic emission over the United States. The recommended scaling for CO and NO_x based on ICARTT by Hudman *et al.* [2007, 2008] (over 50% decrease over ozone season from power plant and industrial sectors and 60% decrease in CO emission over the United States) has not been applied to the standard codes for v8-01-01. (http://acmg.seas.harvard.edu/geos/doc/man/chapter_1.html).

3. OMI-MLS, TES, and GEOS-Chem TCO Data Quality Against Ozonesondes

[13] In this study, comparisons were made between the new version of OMI-MLS TCOs and ozonesondes measurements from IONS-06 in spring and summer 2006. Model values from GEOS-Chem were also evaluated against IONS ozonesondes.

[14] Table 1 shows that the TOMS based OMI-MLS mapped, OMI-MLS interpolated, and OMI-MLS coincident TCOs are smaller than the IONS TCOs on average by 5.9, 5.9, and 5.1 DU (9.9, 10.4, and 9.9 ppb), respectively. It is noteworthy that the mapped OMI-MLS TCOs have a smaller standard deviation of the differences versus IONS, and a substantially better correlation with the IONS measurements in both spring and summer, than the interpolated and coincident TCOs. This indicates the superiority of the

¹Auxiliary materials are available in the HTML. doi:10.1029/2009JD012616.

Table 1. Comparisons of OMI-MLS and GEOS-Chem Tropospheric Ozone Columns With IONS Ozonesonde TCOs for Spring and Summer 2006^a

TCOs	Number of Data	Corr.	Mean Diff.			Std. Dev. of Diff.		
			Column Amount (DU)	Volume Mixing Ratio (ppb)	Percent	Column Amount (DU)	Volume Mixing Ratio (ppb)	Percent
Spring Plus Summer								
Mapped	430	0.65	-5.9	-9.9	-14.5	8.4	14.4	22.5
Interpolated	340	0.43	-5.9	-10.4	-13.9	12.0	20.0	31.8
Coincident	67	0.36	-5.1	-9.9	-10.9	11.4	16.7	29.1
Mapped ^b	312	0.48	-5.3	-9.6	-12.4	10.2	15.7	24.0
Interpolated ^b	242	0.31	-3.5	-7.7	-7.1	14.2	21.2	38.8
Coincident ^b	112	0.26	-4.3	-7.8	-8.0	11.4	16.3	31.2
GEOS-Chem	517	0.77	0.3	-0.2	1.1	6.2	9.9	14.6
Spring								
Mapped	128	0.55	-6.6	-11.9	-18.9	12.7	22.7	36.5
Interpolated	133	0.33	-6.1	-12.1	-15.9	15.6	26.3	43.1
Coincident	27	0.35	-3.4	-9.6	-8.7	14.7	21.9	38.9
Mapped ^b	114	0.48	-2.4	-5.7	-6.8	13.2	22.3	38.1
Interpolated ^b	135	0.28	-1.6	-6.4	-3.1	16.8	24.7	47.7
Coincident ^b	47	0.21	-0.7	-3.6	0.6	13.1	18.0	39.0
GEOS-Chem	168	0.73	-0.7	-1.8	-1.0	5.0	8.6	12.7
Summer								
Mapped	302	0.75	-5.6	-9.0	-12.5	5.6	8.8	13.3
Interpolated	207	0.50	-5.8	-9.3	-12.5	8.9	14.7	21.6
Coincident	40	0.37	-6.1	-10.2	-12.4	8.5	12.6	20.5
Mapped ^b	198	0.57	-7.0	-11.8	-15.7	7.7	9.6	18.6
Interpolated ^b	107	0.40	-5.9	-9.3	-12.1	9.5	15.8	22.3
Coincident ^b	65	0.36	-6.9	-10.7	-14.3	9.3	14.4	22.5
GEOS-Chem	349	0.75	0.8	0.6	2.1	6.6	10.4	15.3

^aThe OMI-MLS mapped, 2-D interpolated, and coincident TCOs are briefed as mapped, interpolated, and coincident, respectively. The tropospheric ozone columns are reported in both column amount (in DU) and volume mixing ratio (in ppb). Corr., correlation coefficients; Diff., differences; Std. Dev., standard deviations; TCOs, tropospheric ozone columns.

^bOMI DOAS total ozone data were used.

mapping product, a conclusion also arrived by *Yang et al.* [2007].

[15] The OMI(TOMS)-MLS TCOs are smaller than their previous retrieval versions [*Yang et al.*, 2007] by ~2 DU. This is indicated both by direct comparisons and by independent comparisons against two different sets of ozonesonde measurements. The most important changes in collection 3 OMI TOMS total column ozone (OMITO3) from the previous version (collection 2) are the improved L1B radiances and cloud top pressures. The effects of these changes vary with latitude and radiative cloud fraction, and according to specific information given in the OMTO3 release (http://jwocky.gsfc.nasa.gov/omi/OMTO3_Release_Details_v8_5.pdf); these changes reduce collection 3 column ozone, relative to collection 2, by ~2.5 DU for a radiative cloud fraction of 0 and by ~5.5 DU for a radiative cloud fraction of 0.3 at 10°N–40°N. The gridded clear sky OMI total ozone data used in computing the new TCO data set are on average ~4 DU (3–6 DU depending on latitude) smaller than the equivalent values used in the earlier version of the TCOs and this is consistent with the differences in collection 3 and collection 2 OMI TOMS total ozone columns for radiative cloud fractions < 0.3. Our independent calculations also agree with *Froidevaux et al.* [2008] that stratospheric columns from version 2.2 MLS data are smaller than the previous version (1.5) by ~1–3 DU depending on latitude. Consequently, OMI-MLS TCOs are ~2 DU smaller than those in previous versions.

[16] Table 1 indicates that OMI(DOAS)-MLS TCOs are larger by 3–4 DU (~6 ppb) than OMI(TOMS)-MLS in spring, but almost no difference in the summer. OMI (TOMS)-MLS TCOs have a more consistent seasonal difference, slightly smaller standard deviations of the differences, and better correlations with the IONS measurements. This analysis was not able to determine whether this is due to the clear sky criterion used in OMI-DOAS total ozone being less effective than the criteria used in OMI-TOMS total ozone or due to the TOMS total ozone products being more effective in detecting tropospheric ozone variations. Because of the apparent superiority of the TOMS OMI-MLS PV mapped product, we shall use the terms OMI-MLS, or OMI-MLS mapped product to refer to that particular product.

[17] The OMI-MLS mapped TCOs for spring and summer 2007 have been directly compared against the OMI(TOMS)-MLS trajectory mapped TCOs from Mark Schoeberl. The OMI-MLS trajectory mapped TCOs (version 1.6) are derived using OMI TOMS collection 3 total ozone and OMI MLS version 2.2 data, based on the methodology described as by *Schoeberl et al.* [2007]. For the trajectory mapped TCOs in the latitude range 15°N–55°N, the values are smaller by 2.0 DU (but larger by just 0.4 ppb in VMR), and the standard deviation of the differences is 8.9 DU (17 ppb). The correlation between the two sets of TCOs is ~0.7. The 2 DU smaller in trajectory mapped TCOs is mostly due to lower tropopause heights of ~4.3 ± 10.6 hPa (one sigma standard deviation) and the differences in the 'effective

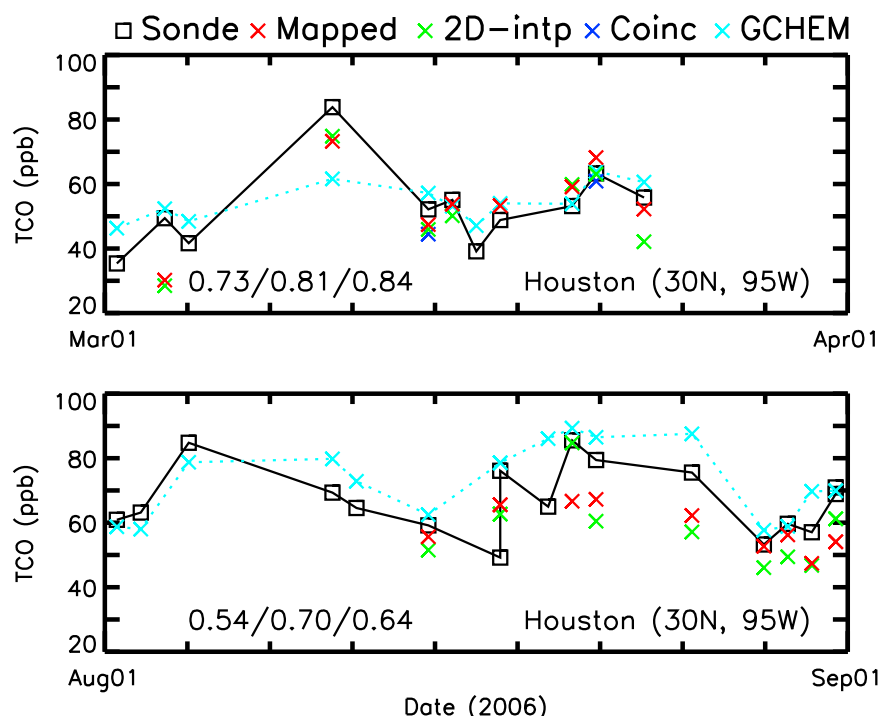


Figure 1. The tropospheric ozone column (expressed as volume mixing ratio, in ppb) from ozonesonde (black squares), GEOS-Chem (cyan crosses), OMI-MLS mapped (red crosses), OMI-MLS 2D interpolated (green crosses), and OMI-MLS coincident (blue crosses) data at Houston ozonesonde station in March and August 2006. The correlation coefficients with IONS TCOs are listed at the left bottom corner in the order of OMI-MLS mapped, OMI-MLS 2D interpolated, and GEOS-Chem TCOs, separated by slashes.

surface pressures' (surface or cloud top pressures). Since column amounts expressed in VMR are not affected by these differences, the offset in the two products is reduced to 0.4 ppb in VMR comparisons with trajectory values slightly larger. Because of the inclusion of time interpolation in the mapping processes, both PV mapped and trajectory OMI-MLS TCOs possess higher correlation coefficients (~ 0.6) and smaller standard deviation of the differences with the sondes than the other techniques. However, the absolute time difference between IONS measurement times and the times corresponding to OMI-MLS mapped TCOs is on average only 2 ± 3 h, and the contribution of these time differences to the ~ 8 DU (14 ppb) standard deviation of the TCO differences is probably small based on calculations of GEOS-Chem and IONS TCO differences with and without time interpolation.

[18] TES TCOs have been compared with TCOs from OMI-MLS for spring and summer 2005 and 2006. The correlation coefficient between OMI-MLS and TES TCOs, are both approximately 0.5. TES TCOs show a high bias of $\sim 10 \pm 12$ DU relative to OMI-MLS TCOs, in the Northern Hemisphere. Nassar *et al.* [2008] showed that TES is biased high throughout the troposphere in the Northern Hemisphere with bias generally in the 0–15% range for the troposphere. According to the mean biases given for TES in Figure 3 of Nassar *et al.* [2008], TES TCOs are high by 2.6 DU, 5.1 DU, and 3.3 DU for the tropics, northern subtropics, and northern midlatitudes, respectively, compared to ozonesondes. This combined with the OMI-MLS low bias of

~ 6 DU accounts for the 10 DU difference between OMI-MLS and TES TCOs.

[19] Comparisons between GEOS-Chem and IONS TCOs show that GEOS-Chem is lower by 0.3 DU (-0.2 ppb) with a small standard deviation of the differences of ~ 6 DU (10 ppb) for spring and summer 2006. The correlation coefficients between GEOS-Chem and sonde TCOs are ~ 0.7 in spring and ~ 0.8 in summer (~ 0.2 higher than those between the mapped TCO products and the sondes for spring). There are larger deviations in the OMI-MLS products than in the GEOS-Chem (versus IONS data), probably because of measurement uncertainties (or variability) in the MLS stratospheric columns, and to a lesser degree, in the OMI total columns, combined with additional uncertainties introduced by mapping the MLS columns to the OMI measurement locations.

[20] As an example, Figure 1 shows time series of different types of TCOs at one of the IONS ozonesonde stations, Houston, for March and August 2006. In general, OMI-MLS and GEOS-Chem TCOs follow the general trend of sonde TCOs, and OMI-MLS TCOs correlate well with sonde TCOs, with correlation coefficients of ~ 0.8 and ~ 0.6 in March and August 2006, respectively. GEOS-Chem, however, tends to be high during August, and it misses the high TCO event on 8 March. Ozone profiles from ozonesondes indicates that the high TCOs on 8 March 2006 is contributed from large ozone enhancement (~ 80 – 90 ppb) above ~ 500 hPa (lower ozone values below ~ 500 hPa (~ 50 – 60 ppb)). While GEOS-Chem overestimates below ~ 500 hPa, it simulates about 10% lower ozone in the mid

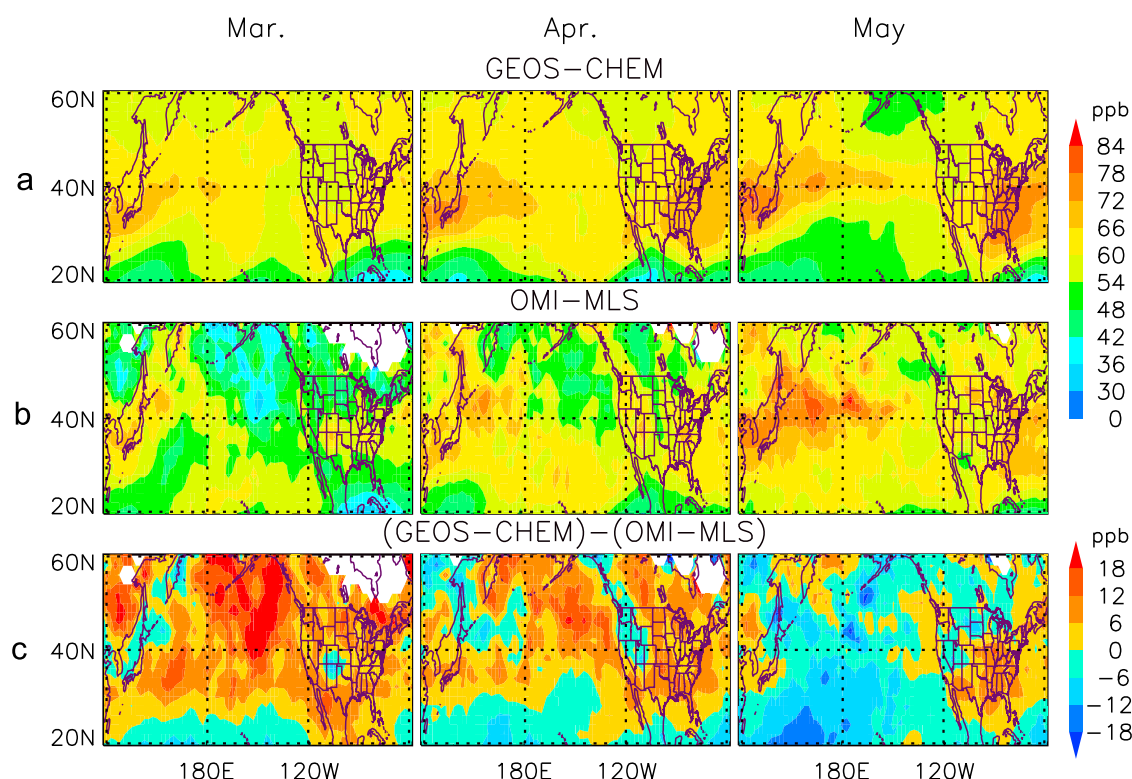


Figure 2. Monthly mean tropospheric ozone columns (expressed as volume mixing ratio in ppb) based on (a) GEOS-Chem, (b) OMI-MLS, and (c) GEOS-Chem minus OMI-MLS mapped columns for (left) March, (middle) April, and (right) May 2005. GEOS-Chem data are in their original model grids of $2^\circ \times 2.5^\circ$ (latitude by longitude) grids, and OMI-MLS residuals are averaged to the same grids as GEOS-Chem data.

and upper troposphere, causing the net underestimation for this high TCO event. The three types of OMI-MLS TCOs perform similarly well. However, it should be noted that the relatively good results for the 2-D interpolated TCOs occur because the MLS orbital track passed near Houston in these comparisons.

4. Monthly Average Distributions

[21] The monthly mean TCO distributions based on OMI-MLS were compared with those from GEOS-Chem simulations for spring 2005 (Figure 2) and 2006 (figure not shown). Good agreement (correlation coefficients range from ~ 0.7 to 0.8) has been found between GEOS-Chem and satellite TCO monthly means in the principal features of their distributions for each month. However, satellite data show more small-scale variability. Over the Pacific, both OMI-MLS and GEOS-Chem show a tongue of enhancement (>66 ppb), which stretches from around the Yellow Sea northeastward into the Pacific, indicating a northeastward advecting feature. This tongue of enhancement extends farther eastward into the Pacific from March to May and increases in their intensity. Over North America, there is a band of TCO enhancement over the eastern North Pacific near the Baja peninsula and an extensive high over the Gulf of Mexico, eastern United States and the adjacent North Atlantic. The East Coast enhancement band (e.g., >60 ppb

in GEOS-Chem data) was relatively narrow in latitude in March. From March to May this band gradually widened and covered more Eastern States and more of the adjacent North Atlantic Ocean (see also *Choi et al.* [2008a, 2008b], who used earlier versions of OMI and MLS retrievals). GEOS-Chem TCO values are higher than OMI-MLS TCOs in March over most of the areas over North Pacific and North America as shown in Figure 2, and this differences decreases to around ~ 10 ppb as indicated in the IONS comparisons in April and over North America in May. In May, GEOS-Chem is lower than OMI-MLS mapped values over most area of North Pacific. Comparisons with ozonesondes indicate that TCOs from GEOS-Chem simulations are more consistent in mean differences relative to IONS data in spring months. While OMI-MLS mapped TCOs have a more negative offset in March (-15 ppb in May versus -11 ppb in April and May) in comparisons to ozonesondes. The relatively smaller OMI-MLS mapped TCOs in March are related to a high bias in the PV mapped ozone in the lower stratosphere during March which might be related to more active dynamics in this region in early spring.

[22] The regional TCO enhancements increased from March to May. Using the Positive Matrix Factorization (PMF) analysis and the GEOS-Chem tagged ozone simulations, *Shim et al.* [2008] concluded that tropospheric ozone production and intercontinental transport of polluted air masses contribute the most to the seasonal ozone increase in

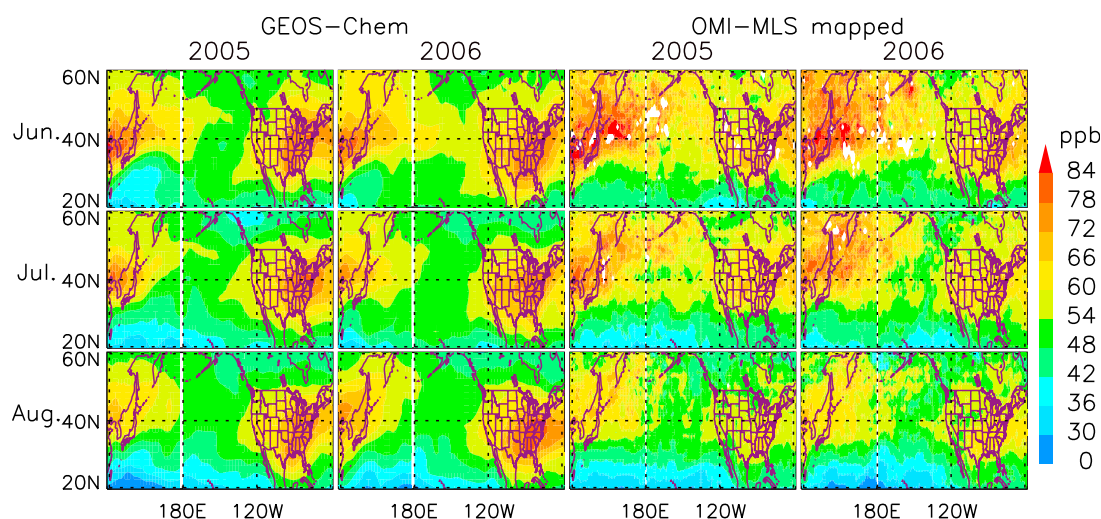


Figure 3. Monthly mean tropospheric ozone columns distributions (expressed as volume mixing ratio, in ppb) based on (left) GEOS-Chem and (right) OMI-MLS mapped columns for (top) June, (middle) July, and (bottom) August 2005 and 2006.

springtime at northern midlatitudes and high latitudes, while the major contribution to ozone variability is from the stratospheric influences and long-range transport of ozone from lower latitudes. Based on 3D model calculations, *Choi et al.* [2008a, 2008b] showed that the stratospheric contribution to TCOs over the eastern United States and the western Atlantic was large in both April and May but that the photochemical production from surface sources of NO_x in the United States began adding significantly to the stratospheric contribution in May.

[23] The summer monthly mean TCOs from GEOS-Chem and OMI-MLS are shown in Figure 3 (in ppb) for 2005 and 2006. From May to June, the area of TCO enhancements shifted further northward over the Pacific, the eastern United States and the adjacent Atlantic. This May to June increase over the northeastern United States was simulated to have been driven by increases in surface NO_x emissions in the eastern United States, together with NO_x being generated by lightning [*Choi et al.*, 2008a].

[24] GEOS-Chem and OMI-MLS mapped monthly mean TCOs have overall monthly correlation coefficients of ~ 0.8 for the Northern Hemisphere in summer 2005 and 2006. The year to year variation in TCOs are small in both model simulations and satellite observations. The dominant features in summer months are the enhancements over the east Pacific and over the eastern United States. OMI-MLS show large TCO values in June 2006 over the west Pacific and the eastern United States, and the observed values decrease in July and August in both years. GEOS-Chem shows similar tendency over the west Pacific; however, this decrease tendency from June to August is not obvious in GEOS-Chem simulations over the eastern United States, even though slight decreasing tendency is present in 2005 simulations. The OMI-MLS TCOs in Figure 5d of *Ziemke et al.* [2006] and the trajectory mapped TCOs also indicate that monthly tropospheric ozone columns peak in June over the eastern United States. GEOS-Chem simulations in this study used the NEI 99 emission inventory over North

America and the scaling of NEI 99 emission inventory recommended by *Hudman et al.* [2007, 2008] has not been used. *Hudman et al.* [2009] concluded that this emission reduction impacts the southeast of United States the most and the mean U.S. boundary layer ozone concentration were reduced by 6–8 ppb over the area during July and August. Ozone profiles from IONS sondes were compared with those from GEOS-Chem simulations for all IONS stations from March to August (see auxiliary material Figure S2), for all IONS stations during July and August, for IONS stations over southeastern United States from March to August (20°N – 40°N , 60°W – 110°W), and for IONS stations over southeastern United States during July and August (see auxiliary material Figure S3). The largest overestimation of GEOS-Chem simulations in the lower troposphere is during July and August over southeast United States. This agrees with the results from *Hudman et al.* [2009], and it explains the relatively high ozone columns over the southeast of United States in the months of July and August leading to less dramatic decrease from June to August over this region. The recommended scaling for CO and NO_x based on work by *Hudman et al.* [2007, 2008] during ozone season for power plant and industrial sectors might be able to reduce this seasonality differences between OMI-MLS and GEOS-Chem TCOs.

[25] OMI-MLS trajectory mapped TCOs (*‘trop_mixt’* data field in Mark’s data set, which is the averaged ozone volume mixing ratio using lapse rate tropopause) also showed increases of TCO enhancements from March to May, and a decrease tendency from June to July (figures not shown). In general, OMI-MLS trajectory mapped TCOs agree with PV mapped TCOs better in summer than in spring and they agree better over North America than over the Pacific. OMI-MLS mapped TCOs showed better agreement with GEOS-Chem in principal distribution feature over the Pacific during spring and summer 2005.

[26] An increase in TCO enhancements from March to May is also present in TES TCOs (figure not shown). The

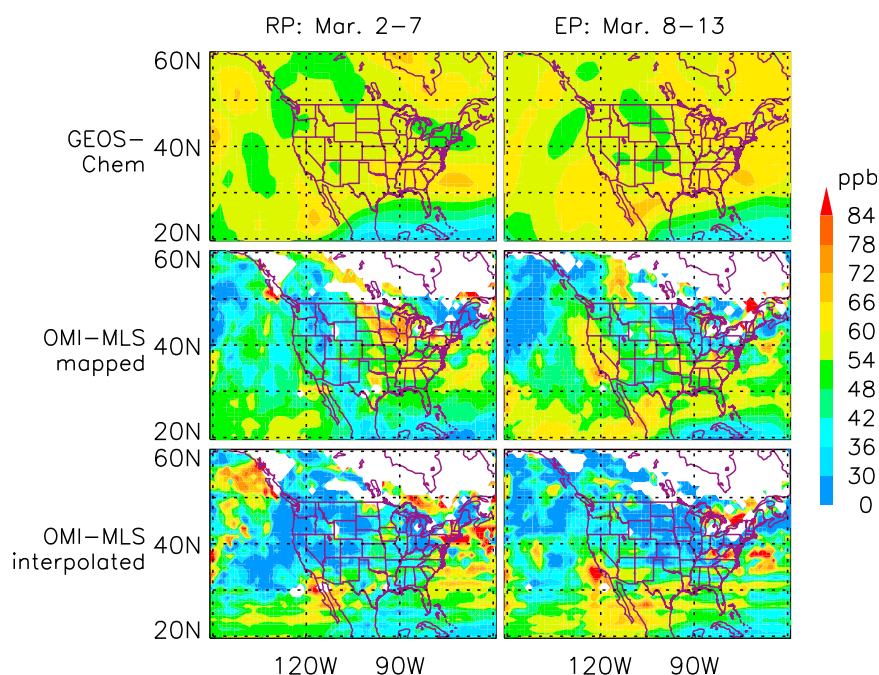


Figure 4. Mean tropospheric ozone columns (expressed in volume mixing ratio, in ppb) during (left) reference period (2–7 March 2005) and (right) enhancement period (8–13 March 2005) using (top) GEOS-Chem, (middle) OMI-MLS mapped, and (bottom) OMI-MLS 2D interpolated TCOs. The longitudinal streaks in the interpolated values may be noted.

monthly means from TES also show month to month TCO change tendencies similar to those seen in OMI-MLS with the intensity of TCO enhancements decreasing slightly from July to August over the west Pacific and the eastern United States.

5. Case Study

[27] Both GEOS-Chem simulations and OMI-MLS data indicate frequent occurrences of TCO enhancements near southern California, the Baja peninsula, and the adjacent Pacific Ocean, and these enhancements sometimes extend northward covering coastal California. Time series autoregressive moving average (ARMA) modeling of OMI-MLS TCO enhancements over the western Pacific (140°E) indicate an occurrence frequency of once every 2.5 days during spring and summer, whereas TCO enhancements over coastal California only occur once every 5 days. On average, it takes 7 days for an Asian pollution outflow to impact the west coast of the United States. Dissipation and/or divergence are likely to lead to such differences in the TCO enhancement frequency. The OMI-MLS TCO enhancement frequencies obtained in this study are new in current literature, however, these are initial results and we will conduct a future study to analysis of the reasons for the obtained time scales.

[28] Previous literatures mostly used OMI-MLS mapped TCOs in monthly average [e.g., Choi *et al.*, 2008a]. To demonstrate that the OMI-MLS mapped TCO could capture enhancements in shorter time scales (weekly rather than monthly), we conducted a spring case study. The case study was selected due to an unusually high TCO enhancement

over Baja peninsula and this enhancement extends to coastal California in spring 2005.

[29] In the second week of March 2005, there was a pronounced TCO enhancement along coastal California and this enhancement was one of the strongest over this region in the spring of 2005, based on both GEOS-Chem and OMI-MLS TCOs. Two 6 day periods were selected for the case study, 2–7 March (reference period) and 8–13 March 2005 (enhancement period), with the enhancement period being associated with a high-TCO event. It should be noted that the duration of the study time periods are constrained by the necessity for relatively clear sky measurements. Therefore, about 6 days were required to provide complete OMI-MLS TCO coverage over North America.

[30] The averaged TCOs for the reference and enhancement periods based on GEOS-Chem and OMI-MLS (TES did not have sufficient data coverage for these periods) are presented in Figure 4. Both OMI-MLS and GEOS-Chem show enhancement tendencies from the reference period to the enhancement period over coastal California and around southern Baja peninsula. The strongest enhancement, based on OMI-MLS, is centered near Santa Barbara, California.

5.1. Stratospheric Intrusion and Wave Breaking

[31] Following Postel and Hitchman [1999] and Scott and Cammas [2002], PV on the 350 K isentropic surface was used to diagnose wave breaking events which are associated with these stratospheric intrusions. The time evolution maps indicate the steepening of a wave crest approximately 2 days before the enhancement period (Figure 5, left). On 8 May (the first day of the enhancement period) at 0000 GMT, a tongue of high PV stretches southeastward, and at 1200 GMT (Figure 5, middle) a high PV cutoff with PV values as high

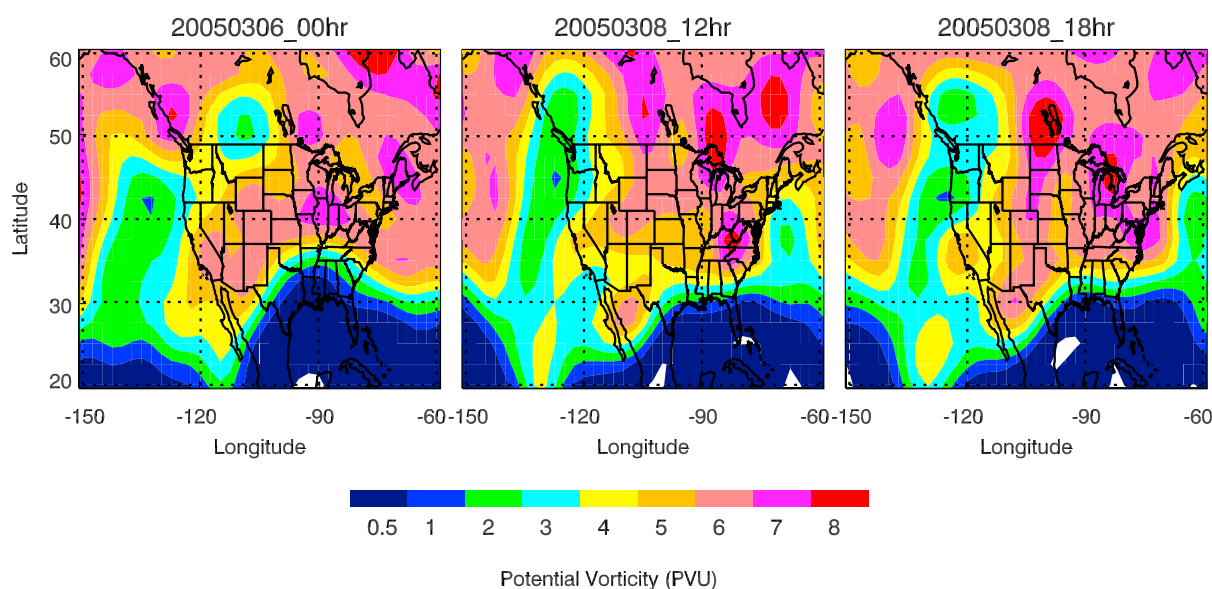


Figure 5. PV contours on the 350 K isentropic surface. PV data were calculated using the 6-hourly NCEP reanalysis data.

as 6 PV units forms beside the wave crest over the Baja peninsula. Six hours later (Figure 5, right), a relatively weak cutoff high shows up over coastal California with the center of PV contours being 1 PV unit larger than the surroundings areas. Therefore, we conclude that stratospheric intrusions associated with wave breaking are present during the TCO enhancement period over the west coast and over the Baja peninsula.

[32] In order to track contributions of stratospheric ozone to the enhancement event, we conducted tagged o_3 simulations [Liu *et al.*, 2002] using GEOS-Chem. Ozone production and loss rates archived from standard GEOS-Chem runs were used to simulate ozone photochemistry in the troposphere. As shown in Figure 6, about 12–15 ppb (20–30%) of TCO enhancements expressed as mean ozone volume mixing ratio have been transported from stratosphere over the coastal California and over the Baja peninsula area. Higher fraction of stratospheric intrusion (25–30%) occurs over southern Baja and over the ocean near California. It is noteworthy to point out that GEOS-Chem tends to underestimate stratospheric intrusions. The transport of ozone from stratosphere to the troposphere in GEOS-Chem is simulated using the synthetic ozone (Synoz) flux boundary condition of McLinden *et al.* [2000], and at some regions the stratospheric intrusion could be a factor 2–3 too low [Hudman *et al.*, 2004]. Nevertheless, the tagged ozone simulation results confirm the stratospheric contributions to the enhancement event over Baja peninsula and over the coastal California.

5.2. Trans-Pacific Transport Influence

[33] Another important mechanism, which could affect the ozone concentrations over the enhancement region, is the trans-Pacific transport. To investigate the possible influence of trans-Pacific transports, 240 h back trajectories were calculated using the Hybrid Single-Particle Lagrangian Integrated Trajectory (HY-SPLIT) model (G. D. Rolph,

Real-time Environmental Applications and Display sYstem (READY) Web site, <http://www.arl.noaa.gov/ready/hysplit4.html>, accessed in 2003; R. R. Draxler and G. D. Rolph, HYSPLIT (HYbrid Single-Particle Lagrangian Integrated Trajectory) Model accessed in 2003 via NOAA ARL READY Web site, <http://www.arl.noaa.gov/ready/hysplit4.html>). The meteorological data used for HY-SPLIT were from the NCEP-reanalysis data set. A back trajectory time of 240 h is considered sufficiently long for identifying the general features of air mass origins [Wang *et al.*, 2003, and references therein].

[34] Four locations on the west coast of the United States (indicated by the triangles in Figure 7), 2 degrees apart in latitude, were chosen to initialize back trajectories every 6h at heights of 2, 4, and 6 km during both periods. The average time for air parcels at 2, 4, and 6 km to cross the Pacific was 6–8 days. The back trajectories initialized at 4 km were most likely associated with the westerlies, whereas trajectories with an initial height of 2 km mostly originated from higher latitudes (40°N–60°N).

[35] Among the 288 trajectories initialized during the enhancement period, on average 25% (31%, 17%, and 25% for those initialized at 2, 4, and 6 km, respectively) of them were found to originate over East Asia (30°N–50°N and 100°E–145°E; 10°N–30°N and 100°E–125°E), compared to only 8% (9%, 5%, 9% for 2, 4, and 6 km, respectively) for those initialized during the reference period. The end point locations after 10 day trajectories are shown in Figure 7. The significantly larger number of trajectories in enhancement period originating from East Asia indicates that the ozone enhancement over coastal California in enhancement period could have been influenced by pollutant emissions from East Asia. The time height cross section of the back trajectories associated with high OMI-MLS TCOs over the west coast (figure not shown) indicates that the trajectories initialized at 2 km (in green) experienced dramatic lifting before they crossed the Pacific. The lifting was driven by

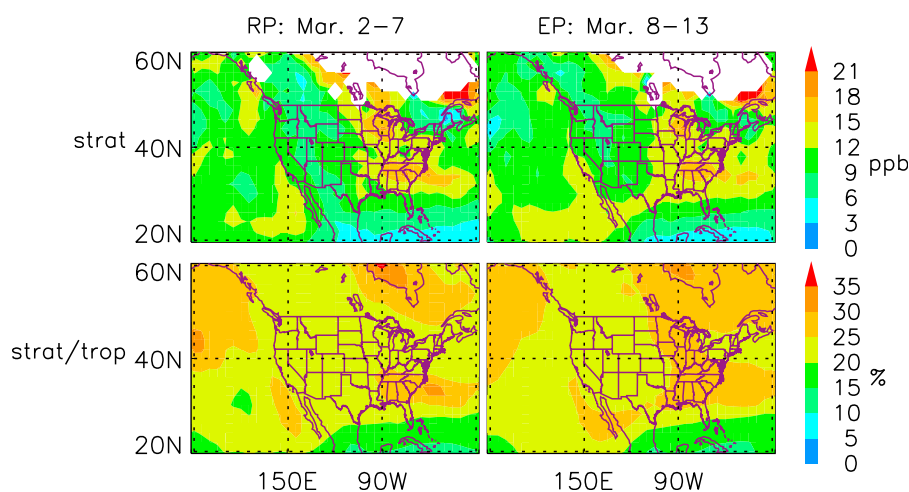


Figure 6. Stratospheric contributions obtained from tagged ozone simulations using GEOS-Chem. (top) Stratospheric contributions (expressed as volume mixing ratio, in ppb) to tropospheric ozone columns (left) for the reference period and (right) for the enhancement period, and (bottom) fraction of stratospheric contribution to the tropospheric ozone columns for the two respective periods.

convection associated with a low-pressure system north of Japan. Associated with the long streak of low-pressure systems over the northern Pacific and the sporadic high-pressure systems located over the southern Pacific, the air parcels were transported rapidly across the Pacific. Associated with the high-pressure system around Washington state, some of the trajectories had a circular shape crossing higher latitudes (up to $\sim 58^\circ\text{N}$) before they arrived over coastal California. The GEOS-Chem simulations indicate elevated CO columns along the trajectory tracks over the North American continent.

[36] A sensitivity run was conducted with Asia anthropogenic emissions turned off 2 months before the case study period. In comparisons with the standard simulation results, there is about 3–6% (~ 2 –3 ppb) of reduction over southern California during the enhancement period, which is about 3–4% higher than those in reference period over the same region.

[37] The 2 day average maps of OMI-MLS mapped TCOs (Figure 8) also provide some additional evidence for the influence of Asian pollution. Figure 8 show TCO enhance-

ment over the middle of the Pacific on 6–7 March (Figure 8, top) and the enhancement propagates westward across the Pacific on 8–9 March (Figure 8, bottom).

6. Summary and Conclusions

[38] Tropospheric ozone columns (TCOs) have been calculated from the differences between the Aura Ozone Monitoring Instrument (OMI) total column ozone and the Aura Microwave Limb Sounding (MLS) measurements of stratospheric ozone (version 2.2). TCOs have been produced using OMI total ozone data sets from both Differential Optical Absorption Spectroscopy (DOAS) algorithm (level 2 collection 3) and Total Ozone Monitoring Spectrum (TOMS) algorithm (level 2 version 3) retrievals. These TCOs have been compared against ozonesonde measurements from the Intercontinental Chemical Transport Experiment (INTEX) Ozonesonde Network Study (IONS) campaign in spring and summer, 2006. The PV mapped TCOs produce higher correlations (~ 0.6 in spring and ~ 0.8 in summer) with the ozonesondes and smaller standard

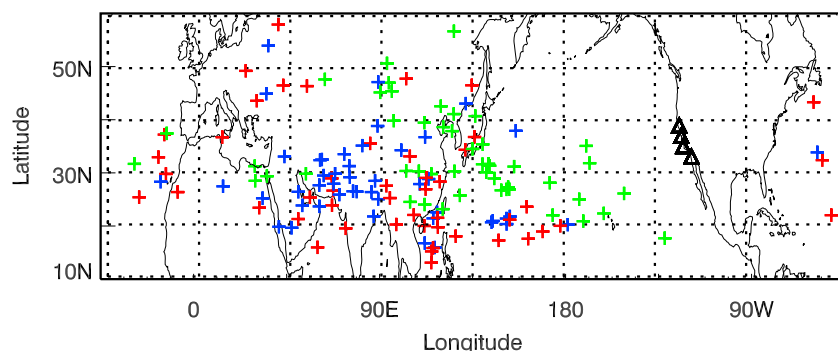


Figure 7. The locations of the end points of the 10 day back trajectories initialized from the west coast of United States (four locations about 2 degrees apart in latitude are indicated by the black triangles). The trajectories were initialized at heights of 2 km (green), 4 km (blue), and 6 km (red).

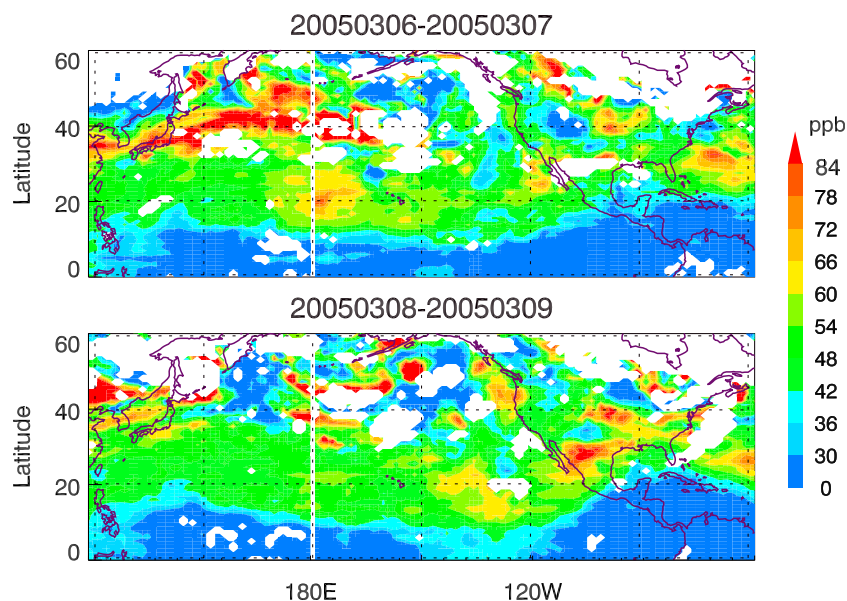


Figure 8. The 2 day mean OMI-MLS mapped tropospheric ozone columns (expressed as volume mixing ratio, in ppb) for (top) 6–7 and (bottom) 8–9 March 2005.

deviations of the differences (~ 13 DU/23 ppb in spring and 6 DU/9 ppb in summer) than simpler approaches (linear interpolation or assumed coincidence). The OMI-TOMS/MLS TCOs are approximately 6 DU (10 ppb in VMR) smaller than the ozonesonde measurements in both spring and summer. In contrast the OMI-DOAS/MLS TCOs are 2 DU (5 ppb) smaller than the sondes in spring but 7 DU (9 ppb) smaller in summer and they are not as well correlated with the sonde variations. The OMI-MLS (from now on meaning the TOMS versions) TCOs are ~ 2 DU (~ 6 ppb) smaller than the previous retrieval version of the TCOs [Yang *et al.*, 2007]. Relative to our PV mapped TCOs, trajectory mapped TCOs (Version 1.6 [Schoeberl *et al.*, 2007]) are smaller by 2 DU between 15°N and 55°N mostly due to the differences in the tropopause heights of 3.5 hPa (1 sigma = 17.3 hPa) and in surface/cloud top pressures since the TCO differences in volume mixing ratio (VMR) are only 0.4 ppb with trajectory mapped TCOs being higher.

[39] GEOS-Chem TCOs show nearly zero offsets relative to the IONS ozonesondes in spring (-1 DU/ -2 ppb) and summer (1 DU/1 ppb) 2006. In spring, but not in summer, the GEOS-Chem TCOs show a slightly larger correlation with the sondes (by ~ 0.2) and a smaller value for the standard deviation of the differences. This is almost certainly related to uncertainties in the MLS stratospheric and OMI total columns as well as uncertainties in mapping the MLS columns to the locations of the OMI column measurements during dynamically active times of year.

[40] Good overall agreement (correlation coefficients range ~ 0.7 to 0.8) has been found between GEOS-Chem and satellite TCO monthly means in the main features of their distributions for spring and summer 2005 and 2006. Areas of OMI-MLS TCO enhancements consist of high values over the west Pacific, eastern North Pacific near the southern California and the Baja peninsula and another high over the Gulf of Mexico, eastern United States and the

adjacent North Atlantic. The OMI-MLS TCO enhancements over the west Pacific and the eastern United States increased from March to June and then decreased. In the GEOS-Chem model, the decrease tendency from June to August is not as dramatic.

[41] A springtime ozone enhancement event over coastal California and over Baja peninsula is presented in the form of 6 day average maps from both satellite and model data. Tagged ozone model simulations confirm the stratospheric contribution to the high TCOs over coastal California and over the Baja peninsula and meteorological fields indicate the stratospheric intrusions are associated with Rossby wave breaking events. Furthermore, back trajectory and comparisons of standard and sensitivity GEOS-Chem simulations with Asia anthropogenic emission turned off provide evidence that the high ozone over coastal California near Santa Barbara, California, has been influenced by cross-Pacific transport. A few day average maps of tropospheric ozone columns from Aura OMI-MLS TCOs also indicate cross-Pacific propagating features.

[42] **Acknowledgments.** We would like to dedicate this paper to Derek Cunnold, who passed away on April 2009. He was a Principal Research Scientist, Acting Chair of School, and Professor at Georgia Institute of Technology's School of Earth and Atmospheric Sciences for 27 years. Derek was an internationally recognized and respected expert regarding the science of the Earth's protective ozone layer, the use of satellite measurements and computer models to study this complex layer, and the interpretation of global atmospheric measurements to determine the sources and sinks of ozone-depleting and greenhouse gases. He was an outstanding mentor for students and young scientists at both Georgia Tech and other institutions. As commented by one of his long-term collaborators, Derek's intelligence, insight, scientific achievements, unselfish service, and quiet, wise, and effective leadership will be deeply missed, but never forgotten, by his many scientific colleagues and admirers around the world. This work has been supported by the NASA Atmospheric Chemistry and Analysis Program (ACMAP). The GEOS-Chem model is managed at Harvard University, and we thank Robert Yantosca and Daniel Jacob for making the model available. We thank KNMI for making the OMI ozone columns available and Pepijn Veefkind for help in interpreting the data.

The TES program is managed at the Jet Propulsion Laboratory, California Institute of Technology, under a contract with the National Aeronautics and Space Administration. We thank Mark Schoeberl for supplying us with his trajectory mapped TCOs. The authors gratefully acknowledge the NOAA Air Resources Laboratory (ARL) for the provision of the HYSPLIT transport and dispersion model and/or READY website (<http://www.arl.noaa.gov/ready.html>) used in this publication. NCEP Reanalysis data were provided by the NOAA/OAR/ESRL PSD, Boulder, Colorado, USA, from their Web site at <http://www.cdc.noaa.gov/>.

References

- Acarreta, J. R., J. F. De Haan, and P. Stammes (2004), Cloud pressure retrieval using the O₂-O₂ absorption band at 477 nm, *J. Geophys. Res.*, **109**, D05204, doi:10.1029/2003JD003915.
- Beer, R. (2006), TES on the Aura Mission: Scientific objectives, measurements and analysis overview, *IEEE Trans. Geosci. Remote Sens.*, **44**, 1102–1105, doi:10.1109/TGRS.2005.863716.
- Bey, I., D. J. Jacob, R. M. Yantosca, J. A. Logan, B. Field, A. M. Fiore, Q. Liu, L. J. Mickley, and M. Schultz (2001), Global modeling of tropospheric chemistry with assimilated meteorology: Model description and evaluation, *J. Geophys. Res.*, **106**, 23,073–23,096, doi:10.1029/2001JD000807.
- Choi, Y., Y. Wang, Q. Yang, D. Cunnold, T. Zeng, C. Shim, M. Luo, A. Eldering, E. Bucsela, and J. Gleason (2008a), Spring to summer northward migration of high O₃ over the western North Atlantic, *Geophys. Res. Lett.*, **35**, L04818, doi:10.1029/2007GL032276.
- Choi, Y., Y. Wang, T. Zeng, D. Cunnold, E. Yang, R. Martin, K. Chance, V. Thouret, and E. Edgerton (2008b), Springtime transitions of NO₂, CO, and O₃ over North America: Model evaluation and analysis, *J. Geophys. Res.*, **113**, D20311, doi:10.1029/2007JD009632.
- Froidevaux, L., et al. (2008), Validation of Aura Microwave Limb Sounder stratospheric ozone measurements, *J. Geophys. Res.*, **113**, D15S20, doi:10.1029/2007JD008771.
- Heald, C. L., et al. (2003), Asian outflow and trans-Pacific transport of carbon monoxide and ozone pollution: An integrated satellite, aircraft, and model perspective, *J. Geophys. Res.*, **108**(D24), 4804, doi:10.1029/2003JD003507.
- Heald, C. L., D. Jacob, R. J. Park, B. Alexander, T. D. Farelle, R. M. Yantosca, and D. A. Chu (2006), Trans-Pacific transport of Asian anthropogenic aerosols and its impact on surface air quality in the United States, *J. Geophys. Res.*, **111**, D14310, doi:10.1029/2005JD006847.
- Holton, J. R., P. H. Hayns, M. E. McIntyre, A. R. Douglass, R. B. Rood, and L. Pfister (1995), Stratosphere-troposphere exchange, *Rev. Geophys.*, **33**, 403–439, doi:10.1029/95RG02097.
- Hudman, R. C., et al. (2004), Ozone production in trans-Pacific Asian pollution plumes and implications for ozone air quality in California, *J. Geophys. Res.*, **109**, D23S10, doi:10.1029/2004JD004974.
- Hudman, R. C., et al. (2007), Surface and lightning sources of nitrogen oxides over the United States: Magnitudes, chemical evolution, and outflow, *J. Geophys. Res.*, **112**, D12S05, doi:10.1029/2006JD007912.
- Hudman, R. C., L. T. Murray, D. J. Jacob, D. B. Millet, S. Turquet, S. Wu, D. R. Blake, A. H. Goldstein, J. Holloway, and G. W. Sachse (2008), Biogenic versus anthropogenic sources of CO in the United States, *Geophys. Res. Lett.*, **35**, L04801, doi:10.1029/2007GL032393.
- Hudman, R. C., L. T. Murray, D. J. Jacob, S. Turquet, S. Wu, D. B. Millet, M. Avery, A. H. Goldstein, and J. Holloway (2009), North American influence on tropospheric ozone and the effects of recent emission reductions: Constraints from ICARTT observations, *J. Geophys. Res.*, **114**, D07302, doi:10.1029/2008JD010126.
- Joiner, J., and A. P. Vasilkov (2006), First results from the OMI rotational Raman scattering cloud pressure algorithm, *IEEE Trans. Geosci. Remote Sens.*, **44**, 1272–1282, doi:10.1109/TGRS.2005.861385.
- Liang, Q., L. Jaegle, D. A. Jaffe, P. WeissPenzias, A. Heckman, and J. A. Snow (2004), Long-range transport of Asian pollution to the northeast Pacific: Seasonal variations and transport pathways of carbon monoxide, *J. Geophys. Res.*, **109**, D23S07, doi:10.1029/2003JD004402.
- Liu, H., D. J. Jacob, L. Y. Chan, S. J. Oltmans, I. Bey, R. M. Yantosca, J. M. Harris, B. N. Duncan, and R. V. Martin (2002), Sources of tropospheric ozone along the Asian Pacific Rim: An analysis of ozonesonde observations, *J. Geophys. Res.*, **107**(D21), 4573, doi:10.1029/2001JD002005.
- Mahlman, J. D. (1997), Dynamics of transport processes in the upper troposphere, *Science*, **276**, doi:10.1126/science.276.5315.1079.
- McLinden, C. A., et al. (2000), Stratospheric ozone in 3-D models: A simple chemistry and the cross-tropopause flux, *J. Geophys. Res.*, **105**, 14,653–14,665, doi:10.1029/2000JD900124.
- Nassar, R., et al. (2008), Validation of Tropospheric Emission Spectrometer (TES) nadir ozone profiles using ozonesonde measurements, *J. Geophys. Res.*, **113**, D15S17, doi:10.1029/2007JD008819.
- Park, R. J., D. J. Jacob, B. D. Field, R. Y. Yantosca, and M. Chin (2004), Natural and transboundary pollution influences on sulfate-nitrate-ammonium aerosols in the United States, *J. Geophys. Res.*, **109**, D15204, doi:10.1029/2003JD004473.
- Pfister, G. G., L. K. Emmons, P. G. Hess, J.-F. Lamarque, A. M. Thompson, and J. E. Yorks (2008), Analysis of the summer 2004 ozone budget over North America using IONS observations and MOZART-4 simulations, *J. Geophys. Res.*, **113**, D23306, doi:10.1029/2008JD010190.
- Postel, G. A., and M. H. Hitchman (1999), A climatology of Rossby waves breaking along the subtropical tropopause, *J. Atmos. Sci.*, **56**, 359–373, doi:10.1175/1520-0469(1999)056<0359:ACORWB>2.0.CO;2.
- Roelofs, G.-J., and J. Lelieveld (1997), Model study of the influence of cross tropopause O₃ transports on tropospheric O₃ levels, *Tellus, Ser. B*, **49**, 38–55, doi:10.1034/j.1600-0889.49.issue1.3.x.
- Schoeberl, M. R., et al. (2007), A trajectory based estimate of the tropospheric ozone column using the residual method, *J. Geophys. Res.*, **112**, D24S49, doi:10.1029/2007JD008773.
- Scott, R. K., and J.-P. Cammas (2002), Wave breaking and mixing at the subtropical tropopause, *J. Atmos. Sci.*, **59**, 2347–2361, doi:10.1175/1520-0469(2002)059<2347:WBAMAT>2.0.CO;2.
- Shim, C., Y. Wang, and Y. Yoshida (2008), Evaluation of model-simulated source contributions to tropospheric ozone with aircraft observations in the factor-projected space, *Atmos. Chem. Phys.*, **8**, 1751–1761.
- Thompson, A. M., et al. (2007a), Intercontinental Chemical Transport Experiment Ozonesonde Network Study (IONS) 2004: 1. Summertime upper troposphere/lower stratosphere ozone over northeastern North America, *J. Geophys. Res.*, **112**, D12S12, doi:10.1029/2006JD007441.
- Thompson, A. M., et al. (2007b), Intercontinental Chemical Transport Experiment Ozonesonde Network Study (IONS) 2004: 2. Tropospheric ozone budgets and variability over northeastern North America, *J. Geophys. Res.*, **112**, D12S13, doi:10.1029/2006JD007670.
- Thompson, A. M., J. E. Yorks, S. K. Miller, J. C. Witte, K. M. Dougherty, G. A. Morris, D. Baumgardner, L. Ladino, and B. Rappenglueck (2008), Tropospheric ozone sources and wave activity over Mexico City and Houston during Milagro/Intercontinental Transport Experiment (INTEX-B) Ozonesonde Network Study, 2006(IONS-06), *Atmos. Chem. Phys.*, **8**, 5113–5126.
- Wang, Y., et al. (2003), Intercontinental transport of pollution manifested in the variability and seasonal trend of springtime O₃ at northern middle and high latitudes, *J. Geophys. Res.*, **108**(D21), 4683, doi:10.1029/2003JD003592.
- Yang, Q., D. M. Cunnold, H.-J. Wang, L. Froidevaux, H. Claude, J. Merrill, M. Newchurch, and S. J. Oltmans (2007), Midlatitude tropospheric ozone columns derived from the Aura Ozone Monitoring Instrument and Microwave Limb Sounder measurements, *J. Geophys. Res.*, **112**, D20305, doi:10.1029/2007JD008528.
- Yienger, J. J., M. Galanter, T. A. Holloway, M. J. Phadnis, S. K. Guttikunda, G. R. Carmichael, W. J. Moxim, and H. Levy II (2000), The episodic nature of air pollution transport from Asia to North America, *J. Geophys. Res.*, **105**, 26,931–26,945, doi:10.1029/2000JD900309.
- Zanis, P., et al. (2003), An estimate of the impact of stratosphere-to-troposphere transport (STT) on the lower free tropospheric ozone over the Alps using ¹⁰Be and ⁷Be measurements, *J. Geophys. Res.*, **108**(D12), 8520, doi:10.1029/2002JD002604.
- Ziemke, J. R., S. Chandra, B. N. Duncan, L. Froidevaux, P. K. Bhartia, P. F. Levelt, and J. W. Waters (2006), Tropospheric ozone determined from Aura OMI and MLS: Evaluation of measurements and comparison with the Global Modeling Initiative's Chemical Transport Model, *J. Geophys. Res.*, **111**, D19303, doi:10.1029/2006JD007089.

P. K. Bhartia, Laboratory for Atmospheres, NASA Goddard Space Flight Center, Greenbelt, MD 20771, USA.

Y. Choi and L. Froidevaux, Jet Propulsion Laboratory, California Institute of Technology, 4800 Oak Grove Dr., Pasadena, CA 91109, USA.

J. Nam, H.-J. Wang, Y. Wang, and Q. Yang, School of Earth and Atmospheric Sciences, Georgia Institute of Technology, 311 Ferst Dr., Atlanta, GA 30332, USA. (qyang@eas.gatech.edu)

A. M. Thompson, Department of Meteorology, Pennsylvania State University, University Park, PA 16802, USA.